

Integrated Lithium Niobate Mach-Zehnder Interferometers for Advanced Modulation Formats

Tetsuya KAWANISHI^{†a)}, Takahide SAKAMOTO^{†b)}, and Akito CHIBA^{†c)}, *Members*

SUMMARY We present recent progress of high-speed Mach-Zehnder modulator technologies for advanced modulation formats. Multi-level quadrature amplitude modulation signal can be synthesized by using parallel Mach-Zehnder modulators. We can generate complicated multi-level optical signals from binary data streams, where binary modulated signals are vectorially summed in optical circuits. Frequency response of each Mach-Zehnder interferometer is also very important to achieve high-speed signals. We can enhance the bandwidth of the response, with thin substrate. 87 Gbaud modulation was demonstrated with a dual-parallel Mach-Zehnder modulator.

key words: optical modulator, quadrature amplitude modulation, lithium niobate, Mach-Zehnder interferometer

1. Introduction

Recently, huge-capacity transmission over 10 Tb/s [1]–[3] was achieved by using differential quadrature-phase-shift-keying (DQPSK) which can provide high spectral efficiency together with enhanced tolerance to chromatic dispersion and polarization mode dispersion [4]–[10]. An integrated lithium niobate (LN) modulator consisting of parallel integrated two small Mach-Zehnder interferometers (MZIs) can be used for high-speed DQPSK signal generation, where the modulation speed can be higher than 40 Gbaud [11], [12]. The integrated modulator is called a dual parallel Mach-Zehnder modulator (DPMZM), which can be also used for single-sideband (SSB) modulation [13], frequency-shift-keying (FSK) [14]–[17], optical frequency sweep [18], [19], etc. In addition, high-speed 16-level quadrature-amplitude-modulation (16-QAM) can be achieved by a quad-parallel MZM (QPMZM) consisting of four MZIs [20], [21]. Parallel MZMs including, DPMZM and QPMZM, can synthesize complicated multilevel optical signals from binary data streams. Thus, to drive the modulators, we can use high-speed electric components designed for binary modulation formats. The number of levels in the optical signal depends on the number of integrated small MZIs (MZI elements, henceforth) embedded in a parallel integrated photonic circuit.

Frequency response of each MZI element is also very important to achieve high-speed signals. The frequency re-

sponse would have a smooth roll-off outside the 3 dB bandwidth of the response, so that the modulator can generate a high-speed optical signal which has a wider spectrum than the 3 dB bandwidth. Over 100 Gbaud optical intensity modulation was demonstrated by using an LN modulator consisting of an MZI [22], [23], where the frequency response over -3 dB point should be very important. Modulator response is limited by velocity mismatch between electric and lightwave signals, and also by response of electrodes, though response of electro-optic (EO) effect in LN is fast enough even for over 100 GHz signal generation. The velocity mismatch can be mitigated by traveling wave electrodes, while the response of electrodes are dominated by loss in material and also by mode-coupling with substrate modes. Frequency response of material loss has smooth roll-off. On the other hand, the mode coupling would have large impact on the response where the signal frequency is higher than the substrate mode cut-off frequency. When the substrate thickness is small, the cut-off frequency would be higher [24], [25]. Thus, this particular loss due to the substrate mode can be suppressed by using thin LN substrate. Precise frequency response measurement is difficult in millimeter-wave region, and measurement techniques themselves would be important research subjects.

This paper is organized as follows. In Sect. 2, the concept of parallel MZMs is described briefly. The total expected bitrate generated by an integrated modulator depends on the number of MZI elements and the frequency response. In Sect. 3, some experimental results of DQPSK and 16-QAM are shown, where multilevel optical signals can be synthesized in integrated parallel MZMs. The modulation speed can be higher than 40 Gbaud with a DPMZM, so that the bitrate can be higher than 80 Gb/s. By using a QPMZM, we can achieve 50 Gb/s transmission where the modulation speed is 12.5 Gbaud. We can expect to achieve a single channel 100 Gb/s transmission using polarization division multiplexing. Section 4 describes discussion on frequency response. A fabricated DPMZM with traveling-wave coplanar waveguide (CPW) electrodes on thin LN substrate can provides enhanced frequency response over 40 GHz. Response in a range from 5 GHz to 63 GHz was measured by using two different methods: electric frequency domain network analyzer technique, and optical spectral measurement of high-speed modulated lightwaves.

Manuscript received November 10, 2008.

Manuscript revised March 11, 2009.

[†]The authors are with National Institute of Information and Communications Technology, Koganei-shi, 184-8795 Japan.

a) E-mail: kawanish@nict.go.jp

b) E-mail: tsaka@nict.go.jp

c) E-mail: chiba@nict.go.jp

DOI: 10.1587/transele.E92.C.915

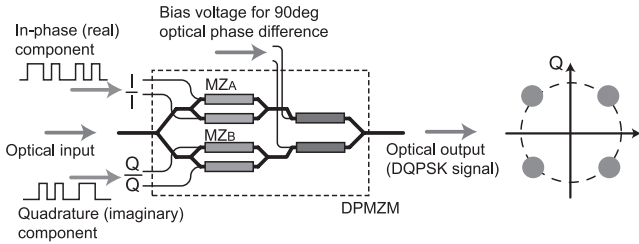


Fig. 1 QPSK using DPMZM.

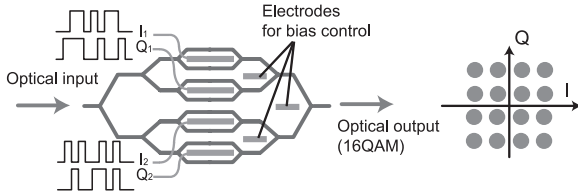


Fig. 2 16-QAM using QPMZM.

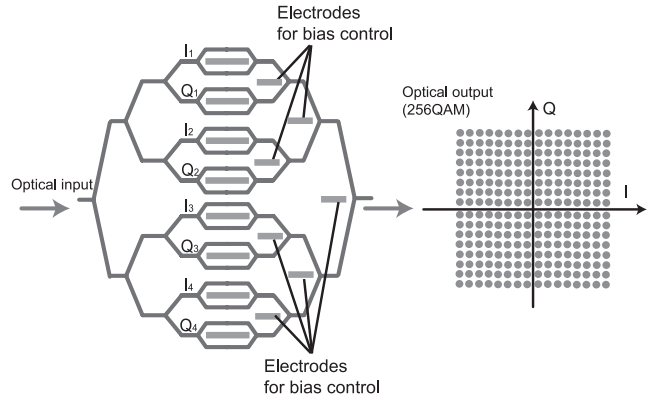


Fig. 3 256QAM using OPMZM.

2. Integrated Modulators for High Data Rate Signal Generation

A DPMZM consists of two MZI elements embedded in a photonic circuit, as shown in Fig. 1. DPMZMs designed for over 40 Gbaud have two high-speed electrodes in each MZI element, in order to achieve push-pull operation on z-cut LN substrate [11]. X-cut substrate with a single high-speed electrode can also provide balanced push-pull operation, however, modulation efficiency is smaller than in z-cut substrate [14]. For DQPSK modulation, two binary data streams are applied to the two MZI elements (MZ_A and MZ_B), to achieve control of in-phase (I) and quadrature (Q) components. Figure 2 shows a schematic of 16-QAM using a QPMZM, where a pair of two-bit codes for in-phase (I_1, I_2) and for quadrature (Q_1, Q_2) components are fed to four MZI elements. While a DPMZM can generate a 2 bit/symbol DQPSK signal from two binary data streams, a QPMZM can achieve 4 bit/symbol from four binary data streams. In general, a parallel MZM with N MZI elements can generate an N bit/symbol lightwave signal from N binary data streams. Bitrate of optical modulated output generated from N electric binary data streams can be expressed by $B = N \times R$ (R : symbol rate). For example, by using an octet-parallel MZM (OPMZM) we can generate 256-QAM from eight binary data streams ($I_1, I_2, I_3, I_4, Q_1, Q_2, Q_3$ and Q_4), where $N = 8$, as shown in Fig. 3.

To achieve high bitrate signal generation, we need integrated modulators with an array of MZI elements ($N \geq 2$) designed for large symbol rate R . To increase the symbol rate R higher than 40 Gbaud, we need flat modulator frequency response up to millimeter wave region where mode coupling between CPW and substrate modes may occur as shown in Fig. 4. The response would have some dips or large loss due to the mode-coupling. When the substrate thickness is small, the cut-off frequency of the substrate mode goes up

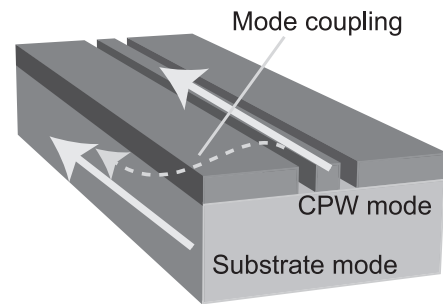


Fig. 4 Undesired mode coupling between CPW and substrate modes.

to high, so that the dips and loss can be suppressed in a millimeter region over 40 GHz. In this work, we focused on integrated LN modulators with two or more MZI elements with thin substrate to increase both N and R for high bitrate optical modulation [24].

3. High-Speed Optical Multilevel Modulation Using DPMZM and QPMZM [4], [20], [21]

For QPSK modulation, a pair of data signals are applied to the two MZI elements in a DPMZM, to achieve control of in-phase and quadrature components [11], [12]. We demonstrated 80 Gb/s DQPSK by using a fabricated DPMZM on a z-cut LN substrate [4], where V_π of each MZI elements was 2.5 V in push-pull operation at low frequency. Optical 3 dB bandwidth of each electrode was larger than 27 GHz. The total optical insertion loss of the packaged modulator was 5.1 dB. The length, width and height of the package were, respectively, 127 mm, 10 mm and 12 mm. Figure 5 shows the experimental setup for DQPSK modulation. As shown in Fig. 1, the DPMZM has two MZI elements (MZ_A and MZ_B). The electrodes A1 and A2 in Fig. 5 are for MZ_A , while B1 and B2 are for MZ_B . The electrodes C1 and C2 are for control of optical phase between the in-phase I and quadrature Q components generated at MZ_A and MZ_B . Each of MZI elements was in a minimum transmission bias point, where optical phase difference between the two MZI elements was adjusted to $\pi/2$ by using the electrode C1 or C2.

A pair of NRZ data streams at 40 Gb/s were obtained

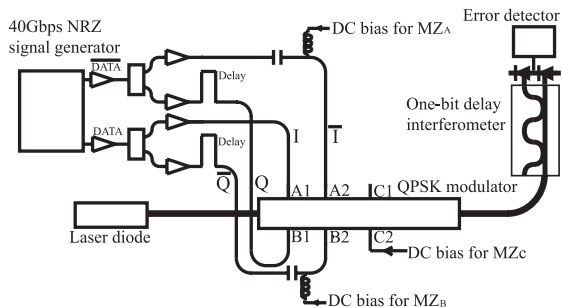


Fig. 5 Experimental setup for DQPSK modulation.

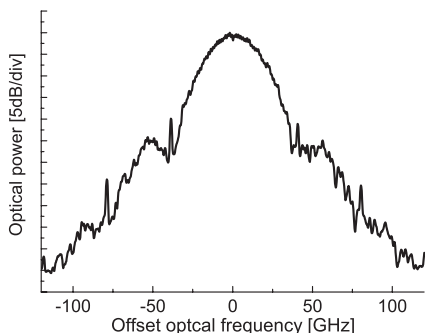


Fig. 6 80 Gb/s optical DQPSK signal.

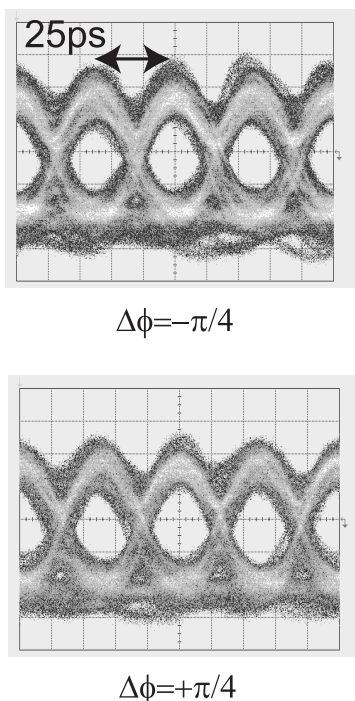


Fig. 7 Eye diagrams of demodulated optical DQPSK signal.

from a 4 : 1 multiplexer that combines four 10-Gb/s sub channels of $2^7 - 1$ pseudo-random-bit-sequence (PRBS). As shown in Fig. 5, one of the streams was fed to MZ_A for I component modulation, and the other was fed to MZ_B for Q component. The amplitude of I and Q signals at the in-

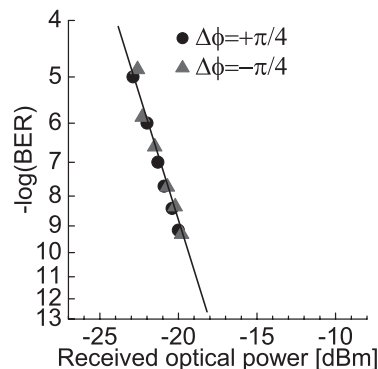


Fig. 8 BER curves of demodulated DQPSK signal.

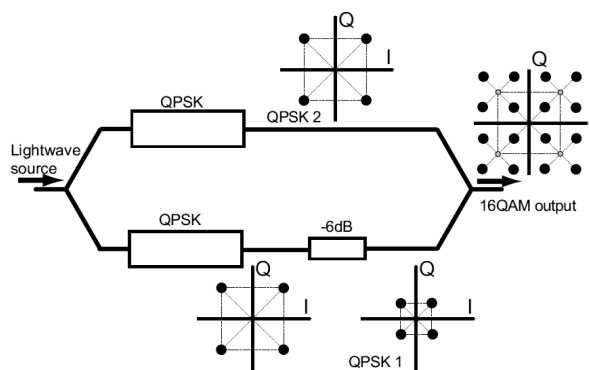


Fig. 9 16-QAM synthesized from two QPSK signals.

put ports of the modulator was 6.5 V (peak-to-peak), corresponding to $2 V_\pi$ at 40 Gb/s, to generate an 80 Gb/s optical DQPSK signal at the output port of the modulator. As shown in Fig. 6, we measured an optical spectrum of a DQPSK signal at the output port of the modulator, without using any optical filters, where full spectral width measured 20 dB down from the maximum of the central wavelength peak was 60 GHz. At the DQPSK demodulator shown in Fig. 5, the DQPSK signal generated at the modulator was decoded by a one-bit delay interferometer whose constructive and destructive ports were connected to a balanced photodetector. We used a single receiver to decode each 40 Gb/s tributary by adjusting the differential optical phase in the one-bit delay interferometer ($\Delta\phi$) at $\pi/4$ or $-\pi/4$. Figure 7 shows eye diagrams measured at the electric output of the balanced photodetector. In back-to-back transmission, clear eye openings were observed for the two tributaries whose symbol rate was 40 Gbaud. We measured a back-to-back BER curve of a sub channel extracted from each tributaries by a 1:4 demultiplexer, as shown in Fig. 8, where the receiver sensitivity at the BER of 10^{-9} was -20 dBm.

By using a QPMZM consisting of two DPMZMs, we demonstrated high-speed 16-QAM [20],[21]. Figure 9 shows principle of optical 16-QAM modulation in our scheme, where the 16 QAM signal can be synthesized by superposing two QPSK signals with different amplitudes. The intensity difference between the QPSK signals is set at

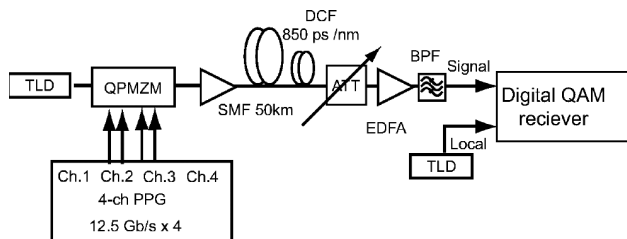


Fig. 10 Experimental setup for 16-QAM using a QPMZM; TLD: tunable laser diode, PPG: pulse-pattern generator, BPF: bandpass filter.

6 dB. The large amplitude QPSK (QPSK 2 in Fig. 9) determines the quadrant where the symbol is mapped, while the small-amplitude QPSK (QPSK 1) fixes the position of the mapping in each quadrant. By the combination of QPSK signals, totally 16 symbols are mapped with equal spacing in a phaser diagram. Note that such a 16-QAM mapping can be achieved from binary data sequences without handling multilevel electric signals.

The QPMZM was fabricated by the hybrid integration of LN waveguide modulators and silica-based planar light-wave circuit (PLC) based couplers [20]. Optical 3 dB bandwidth of each electrode was about 10 GHz. V_{π} of each MZI was 2.9 V. The total optical insertion loss of the fabricated device was 10 dB. Figure 10 shows experimental setup. In the transmitter side, a CW light generated from an external cavity laser diode was 16 QAM modulated with the QPMZM. Each arm of the modulator was push-pull driven with 12.5-Gb/s binary NRZ data with the length of $2^{15} - 1$ PRBS, which was generated from a typically used 4-ch pulse pattern generator, where one DPMZM was driven in the range between $-V_{\pi}$ and V_{π} to generate large-amplitude QPSK. The other DPMZM was driven in the range between $-V_{\pi}/2$ and $V_{\pi}/2$ to generate small-amplitude QPSK. The 16-QAM signal was transmitted over 50-km SMF and demodulated with a QAM receiver. In the QAM receiver, another external cavity laser diode was used as the local oscillator (LO) and frequency detuning between LO and signal was tuned within less than 500 MHz. Carrier phase and data recovery functions were implemented by a so-called off-line processing, i.e. emulated by a numerical computer. Figure 11 shows typical constellation maps of the received QAM signals: (a) back-to-back, (b) 50-km transmitted signals, respectively. With the received power larger than -25 dBm, the bit-error-ratio (BER) was always less than the FEC limit ($\text{BER} = 2 \times 10^{-3}$).

4. Frequency Response of a Fabricated DPMZM with Thin LN Substrate [25]

We fabricated a DPMZM on a thin LN substrate, where the thickness t was 0.1 mm. The thin substrate was bonded on a thick LN substrate with low dielectric adhesive. The DPMZM device used for 80 Gb/s DQPSK shown in the previous section was also measured as a reference, where $t = 1.0$ mm. We measured the modulator response by using

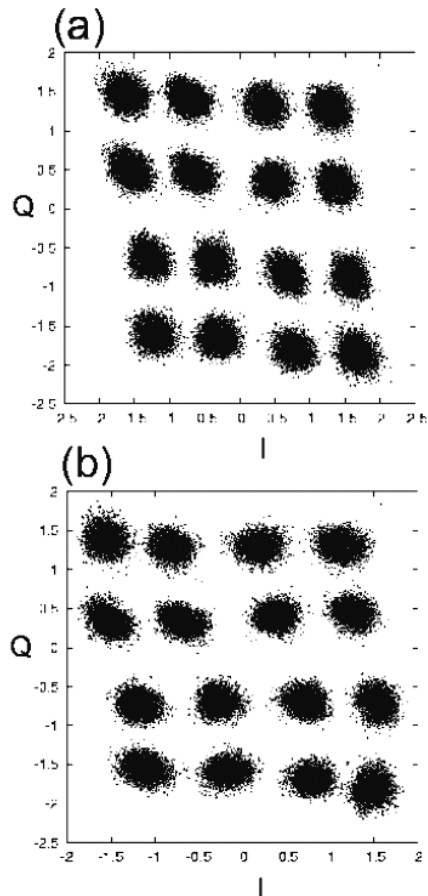


Fig. 11 Constellation maps of 12.5 Gbaud 16-QAM: (a) Back-to-back, (b) 50-km transmitted.

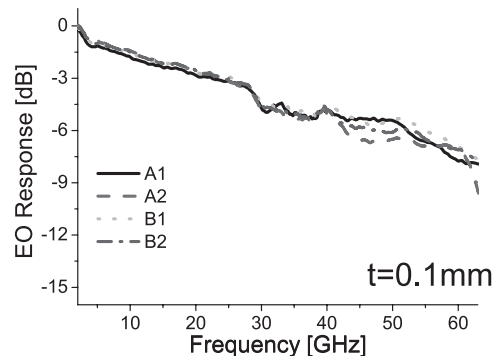


Fig. 12 Modulator frequency response measured by network analyzer based electric domain frequency sweep technique.

a lightwave component analyzer based on millimeter-wave network analyzer technique (Agilent N4373B), as shown in Fig. 12. A1 and A2 denote electrodes on upper and lower arms of MZ_A , while B1 and B2 are upper and lower electrodes of MZ_B . Modulator frequency response can be obtained from the modulated optical signal, where a small sinusoidal electric signal is applied to the modulator. The response uncertainty of the lightwave component analyzer in millimeter region over 50 GHz is ± 2.8 dB. The measured

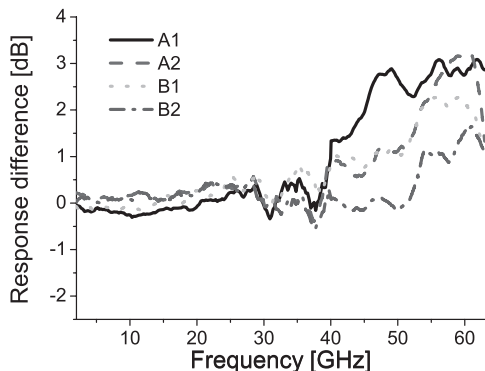


Fig. 13 Response difference between DPMZMs with $t = 0.1$ mm and 1.0 mm.

response at 63 GHz was only 3 dB above the noise floor of the lightwave component analyzer. Thus, we deduce that our measured results in this region would have a few dB uncertainty. Figure 13 shows the response difference between the DPMZMs with $t = 0.1$ mm and $t = 1.0$ mm. When the modulation frequency was higher than 40 GHz, the response for $t = 0.1$ mm was larger than $t = 1.0$ mm, where the difference was 1.5–3.5 dB. The deviation of the difference would be due to the measurement uncertainty or the error in the modulator fabrication. On the other hand, the response difference was very small in a frequency region lower than 40 GHz, where the signal frequency is smaller than the cut-off frequency.

We also measured the modulator frequency response by using an optical spectrum analyzer. A high-speed non-return-to-zero (NRZ) on-off-keying (OOK) electric signal was fed to a pair of electrodes, in order to achieve optical OOK with a single MZI in a DPMZM. The other MZI can be in off-state by adjusting dc bias voltage. Frequency response of the modulator can be estimated from an optical spectrum of the modulated signal. A reference optical spectrum was measured by feeding the same NRZ OOK signal to a reference modulator. Then, we obtained optical sideband intensities for the reference and the modulator under test, as functions of the offset frequency from the optical carrier frequency. Twice the difference between the intensities in dB equals the modulator response difference in dB, because the electric current generated by a photodetector is proportional to the optical power.

We applied a 87 Gbaud binary electric signal to the DPMZM. Figure 14 shows the spectrum of 87 Gbaud optical OOK signal generated by the DPMZM, where a pair of high-speed multiplexer (SHF 408) outputs were directly fed to two electrodes of the DPMZM (A1 and B1). Clear eye opening was achieved, as shown in Fig. 15. We also obtained similar results with electrode A2 and B2 (data not shown). As a reference, we also measured a 87 Gbaud OOK signal generated by the DPMZM with $t = 1.0$ mm. Modulator response difference was calculated from optical spectra for $t = 0.1$ mm and $t = 1.0$ mm, as shown in Fig. 16 (solid line), where the difference measured by the lightwave

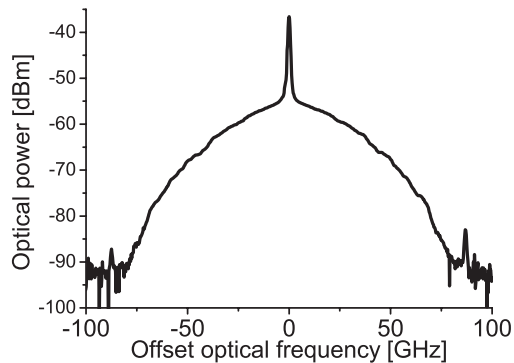


Fig. 14 Optical spectrum of 87 Gbaud optical OOK signal.

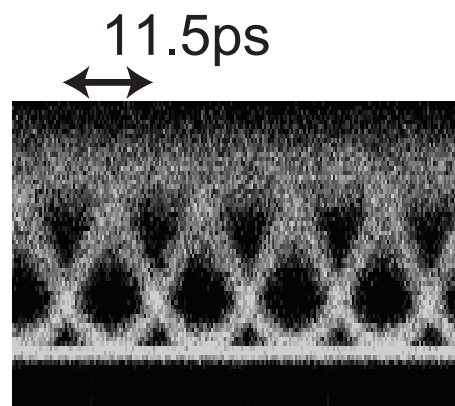


Fig. 15 Eye diagram of a demodulated signal.

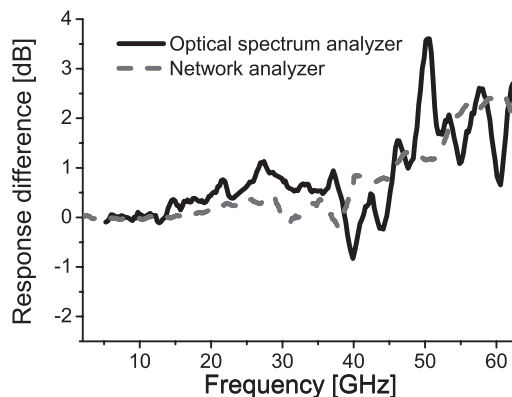


Fig. 16 Modulator response difference was calculated from optical spectra for $t = 0.1$ mm and $t = 1.0$ mm (solid line), and the difference measured by the lightwave component analyzer, (dashed line).

component analyzer, the average of four curves in Fig. 12, was also plotted (dashed line). Both results show that the DPMZM with thin substrate has enhanced response in the millimeter region over 50 GHz, though there is some difference between results by the optical spectrum analyzer and by the network analyzer. Comparison between the two methods may provide us a calibration technique or precise response measurement. If the chirp parameters of the modulator is large and depends on the modulation frequency, the

response measured by the optical spectra would be affected by that of the chirp. However, even if the device structure has asymmetry, the dependence of the chirp parameter on the modulation frequency is small [26].

As shown in Fig. 12, the frequency response for $t = 0.1$ mm had a smooth roll-off in a region from 40 GHz to 63 GHz. The response for $t = 1.0$ mm had excess loss in this region, due to the mode-coupling. Thus, we conclude that the LN modulator with the substrate of $t = 0.1$ mm can suppress the undesired mode-coupling which causes excess loss in modulator response. We note that the optical mode field dimension is smaller than 0.1 mm. Thus, we deduce that the optical insertion loss is not affected by the change of the substrate thickness.

5. Conclusion

Enhanced modulator response in millimeter-wave regime was achieved by using thin LN substrate. High bitrate signals can be generated by a DPMZM or QPMZM with thin substrate, because modulation rate R and the number of MZIs N can be increased simultaneously, where a possible bitrate would be $R \times N$. Clear eye opening was achieved with a fabricated DPMZM ($N = 2$) at $R = 87$ Gbaud.

Acknowledgements

This work was partially supported by NEDO (04A12007) and JSPS (17686032). The authors wish to thank Dr. Hosako of NICT, for his encouragement. They also thank Mr. K. Higuma and Mr. J. Ichikawa of Sumitomo Osaka Cement, Dr. P. J. Winzer of Bell laboratories, Alcatel-Lucent, and Dr. T. Lee of SHF Communication Technologies for fruitful discussion.

References

- [1] A. Sano, H. Masuda, Y. Kisaka, S. Aisawa, E. Yoshida, Y. Miyamoto, M. Koga, K. Hagimoto, T. Yamada, T. Furuta, and H. Fukuyama, "14 Tb/s (140×111-Gb/s PDM/WDM) CSRZDQPSK transmission over 160 km using 7-THz bandwidth extended L-band EDFAs," ECOC2006, Th4.1.1, 2006.
- [2] H. Masuda, A. Sano, T. Kobayashi, E. Yoshida, Y. Miyamoto, Y. Hibino, K. Hagimoto, Y. Yamada, T. Furuta, and H. Fukuyama, "20.4 Tb/s (204 × 111 Gb/s) transmission over 240 km using bandwidth-maximized hybrid Raman/EDFA," OFC/NFOEC2007, PDP20, 2007.
- [3] A.H. Gnauck, G. Charlet, P. Tran, P.J. Winzer, C.R. Doerr, J.C. Centanni, E.C. Burrows, T. Kawanishi, T. Sakamoto, and K. Higuma, "25.6-Tb/s WDM transmission of polarization-multiplexed RZ-DQPSK signals," J. Lightwave Technol., vol.26, pp.79–84, 2008.
- [4] T. Kawanishi, T. Sakamoto, T. Miyazaki, M. Izutsu, T. Fujita, S. Mori, K. Higuma, and J. Ichikawa, "High-speed optical DQPSK and FSK modulation using integrated Mach-Zehnder interferometers," Opt. Express., vol.14, pp.4469–4478, 2006.
- [5] N. Yoshikane and I. Morita, "1.14 b/s/Hz spectrally efficient 50 × 85.4 Gb/s transmission over 300 km using copolarized RZ-DQPSK signals," J. Lightwave Technol., vol.23, pp.108–114, 2005.
- [6] M. Daikoku, I. Morita, H. Taga, T. Tanaka, T. Kawanishi, T. Sakamoto, T. Miyazaki, and T. Fujita, "100-Gb/s DQPSK transmission experiment without OTDM 100G Ethernet transport," J. Lightwave Technol., vol.25, pp.139–145, 2007.
- [7] A.H. Gnauck, P.J. Winzer, S. Chandrasekhar, and C. Dorrer, "Spectrally efficient (0.8 b/s/Hz) 1-Tb/s (25×42.7 Gb/s) RZ-DQPSK transmission over 28 100-km SSMF spans with 7 optical add/drops," ECOC2004, PD, Th4.4.1, 2004.
- [8] R.A. Griffin, "Integrated DQPSK transmitters," OFC 2005, OTuM1, 2005.
- [9] K. Ishida, K. Shimizu, T. Mizuochi, K. Motoshima, D.S. Ly-Gagnon, and K. Kikuchi, "Transmission of 20 × 20 Gb/s RZ-DQPSK signals over 5090 km with 0.53 b/s/Hz spectral efficiency," OFC2004, FM2, 2004.
- [10] T. Kataoka, S. Matsuoka, T. Matsuda, H. Maeda, N. Sakaida, T. Kubo, T. Kotanigawa, and T. Kawasaki, "Field transmission by using a commercially-ready 43 Gbit/s DWDM system employing RZ-DQPSK transponders in high-PMD installed fiber," OFC/NFOEC2007, JThA45, 2007.
- [11] T. Kawanishi, T. Sakamoto, M. Izutsu, K. Higuma, T. Fujita, S. Mori, S. Oikawa, and J. Ichikawa, "40 Gbit/s versatile LiNbO₃ lightwave modulator," ECOC2005, Th2.2.6, 2005.
- [12] T. Kawanishi, T. Sakamoto, and M. Izutsu, "High-speed control of lightwave amplitude, phase, and frequency by use of electrooptic effect," J. Sel. Top. Quantum Electron., vol.13, no.79, pp.79–91, 2007.
- [13] M. Izutsu, S. Shikamura, and T. Sueta, "Integrated optical SSB modulator/frequency shifter," J. Quantum. Electron., vol.17, pp.2225–2227, 1981.
- [14] T. Kawanishi, T. Sakamoto, S. Shinada, M. Izutsu, K. Higuma, T. Fujita, and J. Ichikawa, "LiNbO₃ high-speed optical FSK modulator," Electron. Lett., vol.40, pp.691–692, 2004.
- [15] T. Kawanishi, T. Sakamoto, S. Shinada, M. Izutsu, K. Higuma, T. Fujita, and J. Ichikawa, "High-speed optical FSK modulator for optical packet labeling," J. Lightwave Technol., vol.23, pp.87–94, 2005.
- [16] T. Sakamoto, T. Kawanishi, T. Miyazaki, and M. Izutsu, "Novel modulation scheme for optical continuous-phase frequency-shift keying," OFC2005, OFG2, 2005.
- [17] T. Sakamoto, T. Kawanishi, and M. Izutsu, "Optical minimum-shift-keying with external modulation scheme," Opt. Express., vol.13, pp.7741–7747, 2005.
- [18] T. Kawanishi, T. Sakamoto, and M. Izutsu, "Optical filter characterization by using optical frequency sweep technique with a single sideband modulator," IEICE Electron. Express, vol.3, pp.34–38, 2006.
- [19] T. Kawanishi, T. Sakamoto, and M. Izutsu, "Fast optical frequency sweep for ultra fine real-time spectral domain measurement," Electron. Lett., vol.42, pp.999–1000, 2006.
- [20] T. Sakamoto, A. Chiba, and T. Kawanishi, "50-Gb/s 16-QAM by a quad-parallel Mach-Zehnder modulator," ECOC2007, PDP2.8, 2007.
- [21] T. Sakamoto, A. Chiba, and T. Kawanishi, "50-km SMF transmission of 50-Gb/s 16-QAM generated by quad-parallel MZM," ECOC2008, Tu.1.E.3, 2008.
- [22] P.J. Winzer, G. Raybon, C.R. Doerr, M. Duelk, and C. Dorrer, "107-Gb/s optical signal generation using electronic time-division multiplexing," J. Lightwave Technol., vol.24, pp.3107–3113, 2006.
- [23] T. Kawanishi, T. Sakamoto, A. Chiba, M. Izutsu, and P.J. Winzer, "Duobinary signal generation using high-extinction ratio modulation," OFC2008, OWL2, 2008.
- [24] G.K. Gopalakrishnan, W.K. Burns, and C.H. Bulmer, "Electrical loss mechanisms in travelling wave LiNbO₃ optical modulators," Electron. Lett., vol.28, pp.207–208, 1992.
- [25] T. Kawanishi, T. Sakamoto, A. Chiba, M. Izutsu, K. Higuma, J. Ichikawa, T. Lee, and V. Filsinger, "High-speed dual-parallel Mach-Zehnder modulator using thin lithium niobate substrate," OFC2008, JThA34, 2008.
- [26] T. Kawanishi, K. Kogo, S. Oikawa, and M. Izutsu, "Direct measurement of chirp parameters of high-speed Mach-Zehnder-type optical

modulators,” *Opt. Commun.*, vol.195, pp.399–404, 2001.



Tetsuya Kawanishi received the B.E., M.E. and Ph.D. degrees in electronics from Kyoto University, in 1992, 1994 and 1997, respectively. From 1994 to 1995, he worked for Production Engineering Laboratory of Matsushita Electric Industrial (Panasonic) Co., Ltd. In 1997, he was with Venture Business Laboratory of Kyoto University, where he had been engaged in research on electromagnetic scattering and on near-field optics. He joined the Communications Research Laboratory, Ministry of Posts

and Telecommunications (from April 1, 2004, National Institute of Information and Communications Technology), Koganei, Tokyo, in 1998. In 2004, he was a Visiting Scholar at the Department of Electrical & Computer Engineering, University of California at San Diego, USA. He is now a Senior Researcher of National Institute of Information and Communications Technology, and is currently working on high-speed optical modulators and on RF photonics. He received URSI Young Scientists Award in 1999.



Takahide Sakamoto was born in Hyogo Prefecture, Japan, on May 23, 1975. He received the B.S., M.S. and Ph.D. degrees in electronic engineering from the University of Tokyo, Tokyo, Japan, in 1998, 2000, and 2003, respectively. In 2003, he joined Communications Research Laboratory (now National Institute of Information and Communications Technology), Tokyo, Japan. He has been engaged in all-optical signal processing based on nonlinear optics. His current interest is in electro-optic

devices, such as LiNbO_3 modulators, and their applications to photonic communication systems. Dr. Sakamoto is a Member of the IEEE Lasers & Electro-Optics Society (LEOS).



Akito Chiba received the B.E. in the field of systems engineering, and M.E. and Ph.D. degrees in the field of electronics and information engineering from Hokkaido University, Sapporo, Japan, in 2000, 2002 and 2005, respectively. Since 2005, he has been with National Institute of Information and Communications Technology, Tokyo. His current interest is in electrooptic devices such as LiNbO_3 modulators and their applications to optical communication systems. Dr. Chiba is a member of the

Japan Society of Applied Physics (JSAP) and the Physical Society of Japan (JPS).